Supplemental Data

Mps1 Kinase Promotes Sister-Kinetochore Bi-orientation by a Tension-Dependent Mechanism

Jean-François Maure, Etsushi Kitamura, and Tomoyuki U. Tanaka

Supplemental Results and Discussion

Note 1: GFP-Marked *CEN5* also Showed Frequent Mono-orientation when Mps1 Was Inactivated

The strain used in this experiment (Figure 1A) had *CEN3-tetO*s under the galactose-inducible *GAL1-10* promoter (*PGAL-CEN3-tetO*s), because we also wanted use the same strain in the next experiment (Figure 1B). In Figure 1A, we always cultured the cells in glucose-containing media, i.e., *CEN3* was always active. Nonetheless, we wanted to confirm that our results in Figure 1A were not influenced by the presence of the *GAL1-10* promoter in the vicinity to *CEN3*. To this end, we inserted a *tet* operator array adjacent to *CEN5* but without any further alteration of this centromere (i.e., no regulation by the *GAL1-10* promoter), and we established otherwise the same *MPS1*$^+$ and *mps1-as1* strains as used in Figure 1A. After these strains were treated as in Figure 1A, the majority (about 70%) of GFP-marked *CEN5* showed separation on the bipolar spindle in *MPS1*$^+$ cells but a much lower percentage of separation (about 20%) in *mps1-as1* cells. Most of nonseparated *CEN5* signals located at a spindle pole; they therefore showed mono-orientation on the spindle.

Note that we use the word "mono-orientation" here and in main text with the following definition [S1]. In *monotelic attachment*, one of the sister kinetochores attaches to microtubules whereas the other does not attach to any microtubules. In *syntelic attachment*, both sister kinetochores attach to microtubules extending from one spindle pole. As a result of monotelic or syntelic attachment, sister kinetochores show *mono-orientation*; that is, they are connected to only one spindle pole directly or indirectly.

Note 2: The Bi-orientation Defect in *mps1-as1* Mutant Was Not an Artifact Resulting from Use of *cdc34-2*

We subsequently addressed whether a similar defect in *mps1-as1* could also be found without using *cdc34-2*. To this end, we conducted two experiments as follows. First, we tried to inactivate *mps1-as1* after SPB duplication, for which Mps1 is also required [S2], but before establishment of sister-kinetochore bi-orientation, without using *cdc34-2*. To find the right timing for Mps1 inactivation, we released cells from α-factor arrest and added 1NM-PP1 to inactivate *mps1-as1* at various times (Figure S3). After addition of the inhibitor 45 min after release from α-factor arrest, 69%–71% of *mps1-as1* cells were able to establish a bipolar spindle (i.e., SPB duplication occurred; Figure S3B, red). However, 40%–43% of *mps1-as1* cells showed no sister *CEN3* separation in spite of having a bipolar spindle (Figure S3C, green), a higher percentage than of those not treated with the inhibitor, suggesting a defect in bi-orientation in a subpopulation of cells.

Second, we treated *mps1-as1* cells with nocodazole to disrupt spindle microtubules and then washed it out, allowing cells to reform a bipolar spindle (Figure S4). 1NM-PP1 was added prior to washout of nocodazole to inactivate *mps1-as1*. Because Cdc20 was depleted after the nocodazole washout (and before it), cells did not enter anaphase after reforming bipolar spindle (Figure S4A). *MPS1*$^+$ cells were also treated in the same way as a control. After nocodazole treatment (Figure S4B, 0 min), microtubules were almost completely depolymerized and sister-centromere separation was not found in *MPS1*$^+$ and *mps1-as1* cells. When bipolar spindles were recovered 90 min after nocodazole washout (Figure 4B, 90 min), 71% *MPS1*$^+$ cells, but only 32% *mps1-as1* cells, showed separated *CEN3* GFP dots ($p < 0.0001$; Figure 4C). These results suggest that the bi-orientation defect in *mps1-as1* mutant is also found without using *cdc34-2* and therefore is not an artifact resulting from use of *cdc34-2*.

Note 3: Mps1 Inactivation Leads to Defects in Bi-orientation before Spindles Abnormally Elongate and Become Discontinuous

Did elongated and discontinuous spindles play any causative roles in centromere mono-orientation upon Mps1 inactivation? For example, re-orientation of kinetochore-spindle pole connections may become less efficient because of a longer distance between two poles or discontinuity of the spindle. We first observed how these abnormal spindles occurred in *mps1-as1* cells, by using live-cell imaging, when the cells were released from *cdc34-2* arrest and rearrested by Cdc20 depletion (Figure S1; data not shown). The length of spindles gradually became larger at later time points (Figure S1C). After spindles elongate, they gradually became sparse (i.e., microtubule signals became weak between the two spindle poles) and even discontinuous in the middle. The frequency of discontinuous spindles increased up to 25% during our observation (Figure S1B).

Although the majority of spindles became sparse and discontinuous after a prolonged arrest (>2 hr after release from *cdc34-2* arrest) by Cdc20 depletion, many bipolar spindles still had abundant microtubule signals during our observation (<2 hr after release from *cdc34-2* arrest). Thus, appearance of sparse and discontinuous spindles might have occurred more slowly than that observed by Jones et al. [S3] (they reported that virtually all spindles became sparse and discontinuous in *mps1-as1* cells). This possible discrepancy, if it exists, might be due to the method used for observation. In fact, we observed abnormal spindles less frequently with live-cell imaging (used for Figure 1A and Figure S1) than in fixed cells (used by Jones et al. [S3]).

To address whether elongated or sparse/discontinuous spindles played any causative roles in centromere mono-orientation upon Mps1 inactivation, we observed

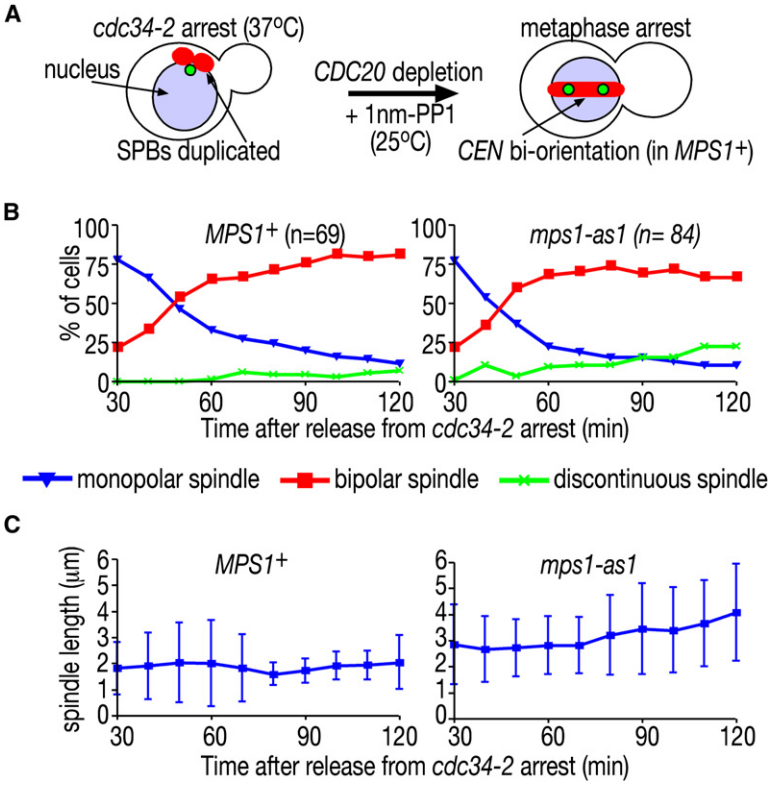

Figure S1. Observation of the Mitotic Spindles after Mps1 Is Inactivated upon Release from *cdc34-2* Arrest

Supplement to Figure 1A. *MPS1*$^+$ (T4195) and *mps1-as1* (T4174) cells with *PGAL-CEN3-tetOs TetR-GFP YFP-TUB1 cdc34-2 PMET3-CDC20* (*PGAL* and *PMET3* stand for the *GAL1-10* promoter and the *MET3* promoter, respectively) were treated as in Figure 1A.

(A) Schematic showing how cells were treated. Note that, in *cdc34-2* arrest, SPBs are duplicated but not yet separated, and DNA replication is not yet initiated [S3, S56]. In metaphase arrest (Cdc20 depletion), a bipolar spindle is formed, and sister centromeres separate frequently on the spindle (in *MPS1*$^+$ cells: see Figure 1A).

(B) Graphs show the percentage of cells with a monopolar spindle (SPBs not yet separated; blue), a bipolar spindle (SPBs are separated; red), and discontinuous spindles (i.e., those in which microtubule signals are discontinuous somewhere between two spindle poles; green).

(C) Graphs show the length of the bipolar spindles (mean ± SD) at each time point.

centromere behavior soon after establishment of the bipolar spindle in *MPS1*$^+$ and *mps1-as1* cells. In the representative *MPS1*$^+$ cell shown in Figure S5A, sister *CEN3*s have transiently separated 1 min after bipolar spindle establishment and showed continuous separation at 3 min and onward. In the representative *mps1-as1* cell, the spindle length was similar to, or only slightly longer than, the *MPS1*$^+$ cell within 5 min after bipolar spindle establishment, but sister *CEN3*s never separated on the bipolar spindle. We studied whether sister *CEN3* dots separate immediately upon bipolar spindle establishment (0 min) and 1 min after it (Figure S5B) in a number of cells; a considerable number of *MPS1*$^+$ cells (0 min, 9/63; 1 min, 12/63) showed sister *CEN3* separation, whereas such separation was never found in *mps1-as1* cells (0 min, 0/69; 1 min, 0/69). At 0 min, the average spindle length was almost the same in *MPS1*$^+$ and *mps1-as1* cells. At 1 min, the spindle length distributions of the two strains overlapped considerably. At these time points, sparse/discontinuous spindles were rarely found in *MPS1*$^+$ or *mps1-as1* cells. We concluded that *mps1-as1* cells showed defects in bi-orientation

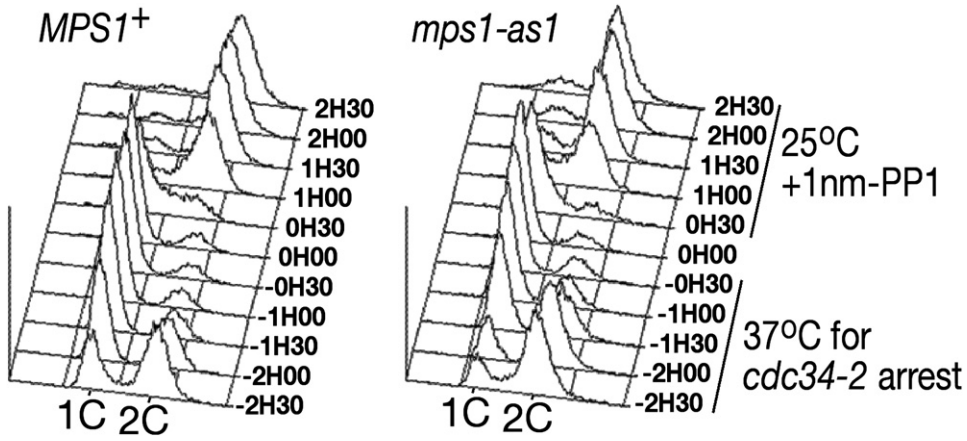

Figure S2. When Mps1 Is Inactivated, Cells Undergo DNA Replication Normally

MPS1$^+$ (T4384) and *mps1-as1* (T4356) cells with *cdc34-2 PMET3-CDC20* (see Figure 2A for complete genotypes) were incubated in methionine dropout medium at 37°C for 2.5 hr, leading to arrest because of *cdc34-2*. Subsequently they were incubated at 25°C (to release cells from *cdc34-2* arrest) in YP medium, containing 10 μM 1NM-PP1 (to inactivate *mps1-as1*) and additional 2 mM methionine (to deplete Cdc20). During these culture processes, cells were sampled and fixed with ethanol every 30 min and subjected to FACS DNA content analyses. Time 0 is defined as the start of culture at 25°C.

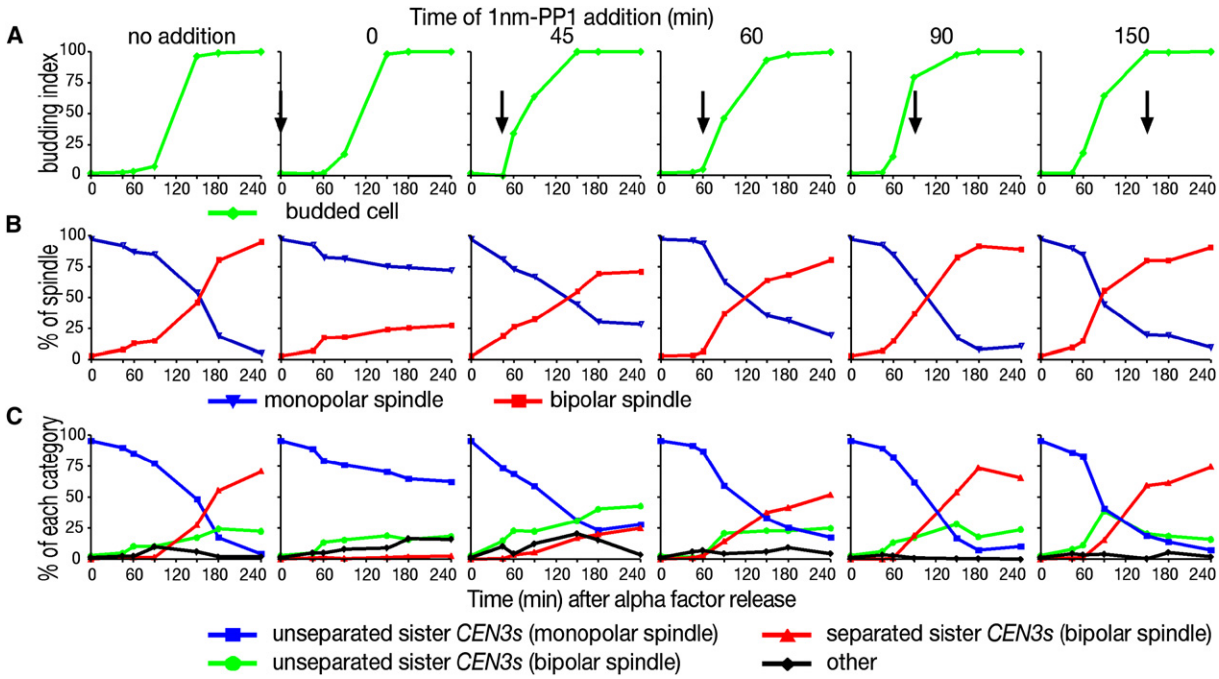

Figure S3. Mps1 Inactivation Causes Bi-orientation Defects after Release from α Factor Arrest

mps1-as1 PGAL-CEN3-tetOs TetR-GFP YFP-TUB1 PMET3-CDC20 cells (T3869) were incubated in methionine dropout medium containing α factor. After 3 hr, they were washed (defined as time 0) and split into six cultures in YP medium containing 2 mM methionine (to deplete Cdc20). At time 0, 45, 60, 90, and 150 min, 10 μM 1NM-PP1 was added to each culture to inactivate *mps1-as1*. In one culture, 1NM-PP1 was not added (no addition) as a control. All media contained glucose, which kept *CEN3* always active during the experiment. Samples were fixed with paraformaldehyde at time points indicated in the graphs.

(A) Graphs show the percentage of cells with buds (green). Arrows indicate timing of 1NM-PP1 addition.

(B) Graphs show the percentage of cells with monopolar (blue) and bipolar (red) spindles.

(C) Graphs show the percentage of cells with unseparated sister *CEN3*s on monopolar (blue) and bipolar (green) spindle, and separated sister *CEN3*s on bipolar spindle (red).

before abnormal spindle elongation and discontinuity, which therefore cannot be the sole reason for centromere mono-orientation.

Rather, we suspect that the abnormal spindles are the outcome of extensive centromere mono-orientation in *mps1-as1* cells. Consistent with this notion, bi-oriented sister kinetochores on the metaphase spindle seem to limit the length of metaphase spindle to the normal level. Indeed, cohesion between sister chromatids is necessary for this limitation [S4], probably by resisting the force to elongate the spindle length, which is generated between antiparallel microtubules that extend from the opposite poles and overlap at the middle of the spindle [S5].

Note 4: Once Sister-Kinetochore Bi-orientation Is Established, It Is Maintained after Mps1 Is Inactivated

Mps1 is necessary to establish sister-kinetochore bi-orientation; then, once bi-orientation is established, is Mps1 still required for its maintenance? To test this, we arrested *MPS1*$^{+}$ and *mps1-as1* cells in metaphase by shutting off expression of Cdc20 (under control of *MET3* promoter). As a control, we also treated the *ask1-3* mutant, which is defective in maintenance of bi-orientation at the restrictive temperature, in the same way (*ask1-3* behaves similarly to *spc34-3* [S6]; both Ask1 and Spc34 are components of the Dam1 complex that is a kinetochore subcomplex in metaphase [S7]). When Cdc20 was depleted in these three strains at the permissive temperature without 1NM-PP1, sister *CEN3*s marked with GFP were found separated in 67%–82% of cells (Figure S6); centromere bi-orientation was therefore established in the majority of cells. We then shifted the temperature of the cell culture to 37°C and simultaneously added 1NM-PP1 to inactivate both *mps1-as1* and *ask1-3* in the same culture conditions. After 45 min, the percentage of separated *CEN3* on the bipolar spindle decreased to less than 10% in *ask1-3* cells, whereas the percentage remained almost constant in *MPS1*$^{+}$ and *mps1-as1* cells (Figure S6). We cannot make a definite conclusion that Mps1 is not required for maintenance of bi-orientation once it is established, because *mps1-as1* treated by 1NM-PP1 may still have residual Mps1 function. Nonetheless, the result makes a sharp contrast with the extensive mono-orientation, shown in Figure 1A. Thus, Mps1 might not be required for maintenance of bi-orientation once it is established. We previously obtained a similar result for Ipl1: i.e., by using *ipl1-321* temperature-sensitive mutants, we found that bi-orientation was still maintained in metaphase-arrested cells after the temperature of the cell culture was shifted to 37°C [S8].

Note 5: Studying Tension-Dependent Bi-orientation by Making an Unreplicated Dicentric Minichromosome

To facilitate sister-kinetochore bi-orientation on the metaphase spindle, syntelic attachments must be either

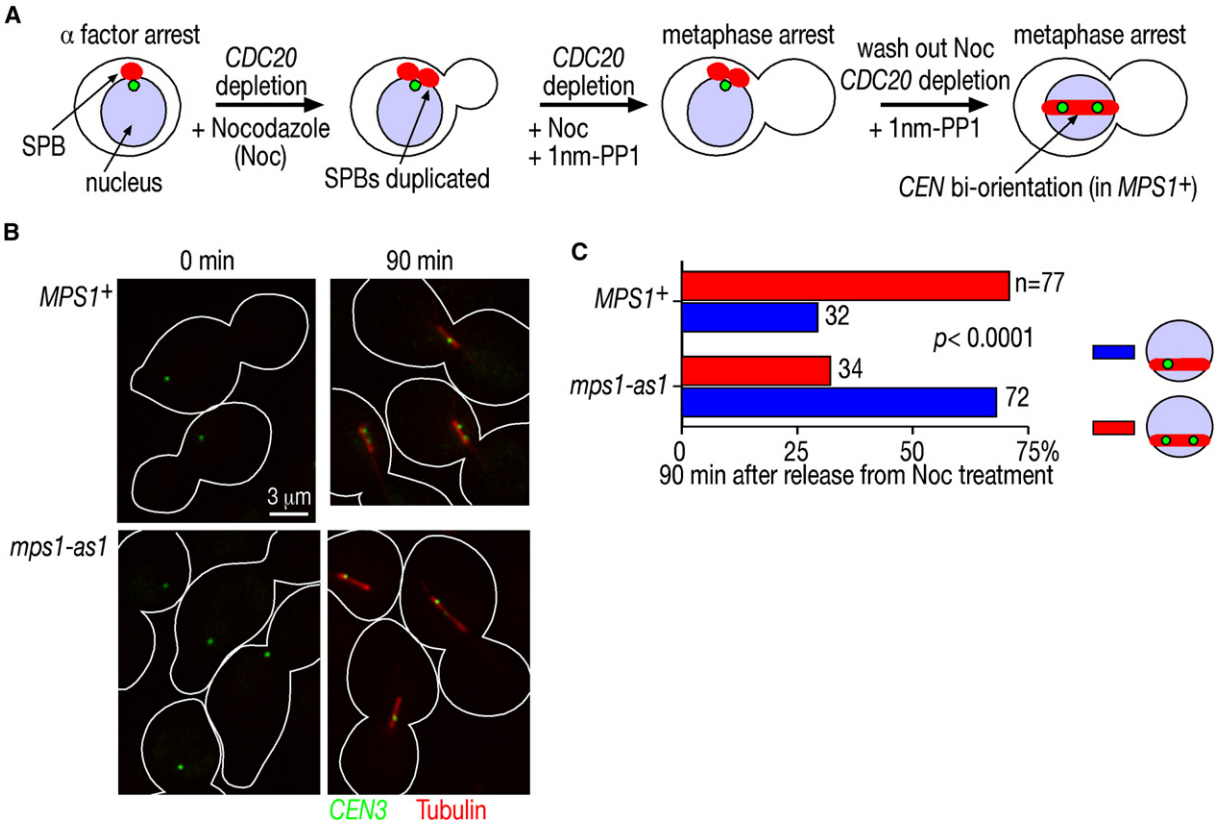

Figure S4. Mps1 Inactivation Causes Bi-orientation Defects after Nocodazole Treatment and Subsequent Washout

MPS1$^+$ (T3531) and *mps1-as1* (T3869) cells with *PGAL-CEN3-tetOs TetR-GFP YFP-TUB1 PMET3-CDC20* were incubated in methionine dropout medium containing α factor. After 2.5 hr, they were washed and cultured in YP medium containing 2 mM methionine (to deplete Cdc20) and nocodazole (30 μg/ml; to depolymerize microtubules). 1NM-PP1 (10 μM; to inactivate *mps1-as1*) was added when 70% cells showed bud emergence. Subsequently, nocodazole was washed out (defined as time 0), 90 min after addition of 1NM-PP1. Cells were further incubated in YP medium containing 2 mM methionine and 1NM-PP1 for recovery of microtubules. All media contained glucose, which kept *CEN3* always active during the experiment. GFP and YFP images were acquired at time 0 and 90 min.

(A) Schematic showing how cells were treated.

(B) Images of representative cells. White lines outline cell shapes. Scale bar represents 3 μm.

(C) Graphs show the percentage of cells with bipolar spindle, which has separated GFP signals (red) and a nonseparated signal (blue).

avoided or corrected [S1]. Avoidance could be dependent on the back-to-back sister-kinetochore geometry such that they face in opposite directions. Error correction, by contrast, is thought to stem from stabilization of kinetochore-spindle pole connections by tension, arising from bi-orientation but not syntelic attachment [S9, S10]. To investigate the error-correction mechanism, we previously developed an unreplicated circular minichromosome harboring two centromeres [S10]. The two centromeres on this minichromosome are not sisters born from DNA replication; therefore, the geometry mechanism would not work. However, tension-dependent error correction should still work as they are connected by chromatin DNA. Because such an unreplicated minichromosome is extremely unstable for transmission to daughter cells upon cell division, we generated it by a two-step induction procedure from a stably transmitted minichromosome, as illustrated in Figure 3A [S10]; we placed the sole replication origin (ARS) of this minichromosome between two recombination sites [S11] and shut off the second centromere by placing it under control of the galactose inducible *GAL1-10* promoter [S12]. We first removed the replication origin by inducing recombinase [S11] from the *MET3* promoter, and subsequently activated the second centromere by shutting off the *GAL1-10* promoter. The minichromosome was visualized by the insertion of a *tet* operator array bound by TetR-GFP [S13]. In wild-type cells, the two centromeres on this unreplicated dicentric minichromosome always bi-oriented efficiently [S10], suggesting that a tension-dependent mechanism suffices for their bi-orientation.

Note 6: Studying Kinetochore Detachment from a Spindle Pole by Making Cells with Four SPBs and an Unreplicated Minichromosome

If Mps1 is indeed involved in a tension-dependent error-correction mechanism, we may see the role of Mps1 in detaching a centromere from one SPB and attaching it to another SPB when tension is not applied on this centromere-SPB connection. This re-orientation should occur with unreplicated monocentric minichromosomes during metaphase. However, such re-orientation was relatively low (about 10% in the condition used in

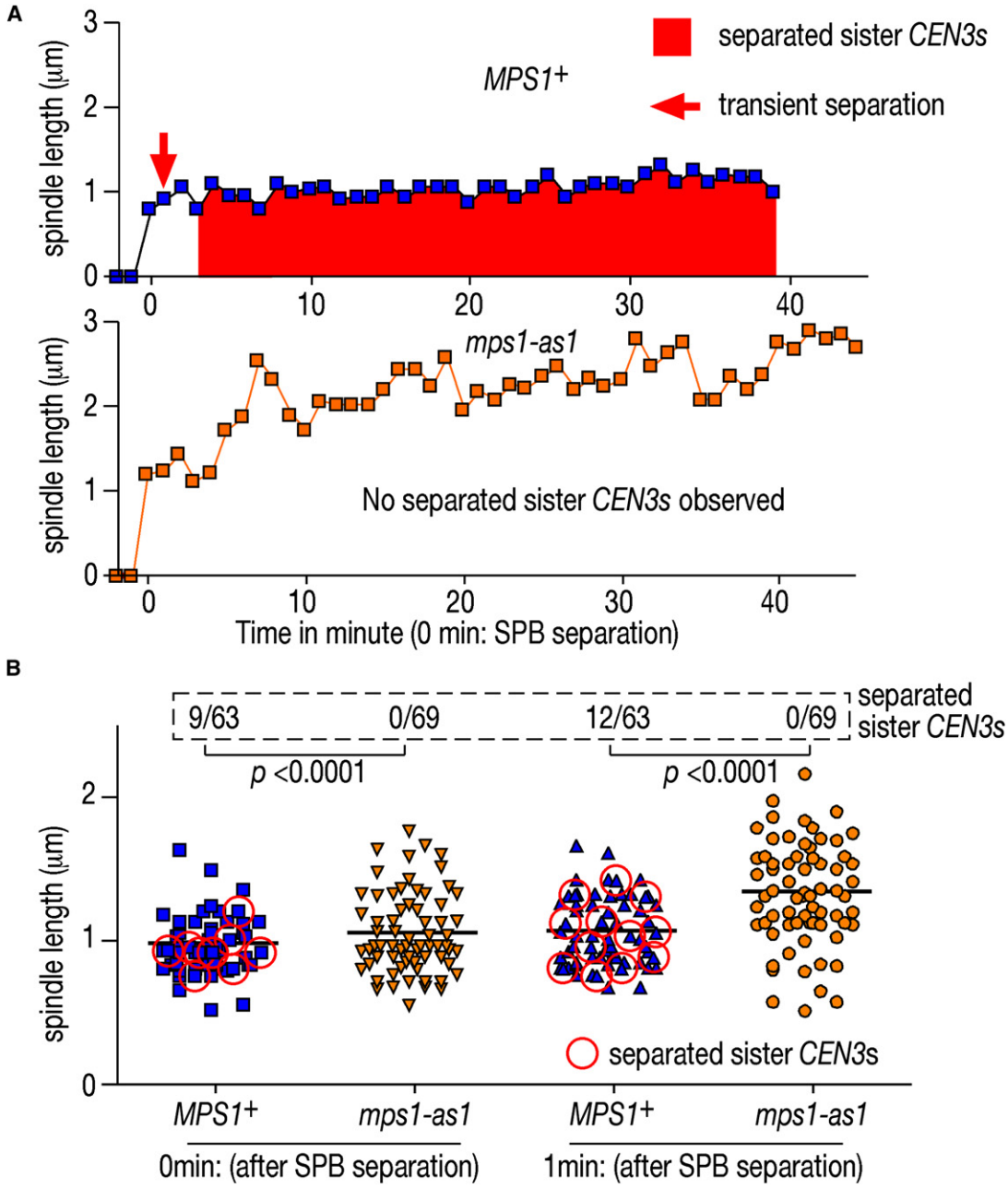

Figure S5. When Mps1 Is Inactivated, Bi-orientation Defects Become Evident before the Bipolar Spindle Elongates Abnormally

MPS1$^+$ and *mps1-as1* cells (T4195 and T4174, respectively; see Figure 1A) were treated and images were acquired, as in Figure 1A.

(A) In a representative *MPS1*$^+$ (top) and *mps1-as1* (bottom) cell, the length of the spindle is plotted against time (0 min; establishment of bipolar spindle, i.e., the first time point at which SPB separation was observed), and sister *CEN3* separation is marked in red (an arrow, and an area below the line). Note that sister *CEN3* separation was not found in the *mps1-as1* cell during observation.

(B) The length of the spindle is plotted in *MPS1*$^+$ (blue) and *mps1-as1* (orange) cells, 0 and 1 min after bipolar spindle establishment. A red circle indicates a cell showing separated sister *CEN3*s on the spindle. A black line shows the mean of the spindle length in each group. Note that sister *CEN3* separation was found in none of the *mps1-as1* cells at these time points.

[S10]) between two SPBs, even in *MPS1*$^+$ cells, probably because the minichromosome often returned rapidly to the original SPB after it detached, rather than changing its SPB partner. To increase the chance of detecting re-orientation between different SPBs, we observed the movement of unreplicated monocentrics in cells containing four instead of two SPBs [S10]. Under this circumstance, three rather than one SPBs competed with the SPB currently in possession of the minichromosome. We created cells with four SPBs, as illustrated in Figure 4A [S10]; by using the *GAL1-10* promoter, we expressed a mutant of cohesin Scc1 that is resistant to cleavage by separase [S14]. These haploid cells failed to segregate chromosomes, but re-entered the next cell cycle because they lacked *BUB2* gene, which would have otherwise blocked the exit from mitosis of those

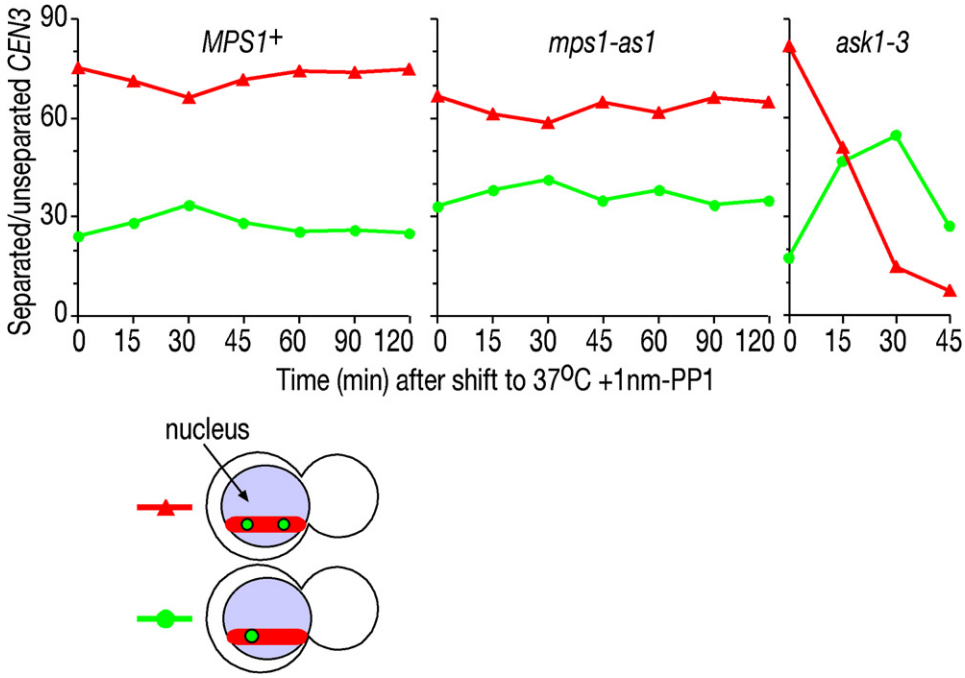

Figure S6. Once Sister-Kinetochore Bi-orientation Is Established, It Is Maintained after Mps1 Is Inactivated

MPS1$^+$ *ASK1*$^+$ (T3531), *mps1-as1* (T3869), and *ask1-3* (T2997) cells with *PGAL-CEN3-tetOs TetR-GFP YFP-TUB1 PMET3-CDC20* cells were incubated in YP medium containing additional 2 mM methionine (to deplete Cdc20) at 25°C. After 3.5 hr, they were incubated at 37°C in the same medium but containing 10 μM 1NM-PP1 (to inactivate both *mps1-as1* and *ask1-3*). All media contained glucose, which kept *CEN3* always active during the experiment. Time 0 is defined as the start of culture at 37°C. Samples were fixed with paraformaldehyde at time points indicated in the graphs. GFP and YFP images were acquired from fixed cells. Graphs show the percentage of cells with nonseparated (green) and separated (red) sister *CEN3*s on the bipolar spindle, in which tubulin signals are continuous between two spindle poles. We did not score sister *CEN3* separation at 60 min or later in *ask1-3* cells because in the majority of them, tubulin signals were not continuous between two spindle poles at these time points.

cells whose SPBs had not entered the buds [S15]. Reduplication of chromosomes and SPBs during the next cell cycle created diploid nuclei with four (or three when two of them are fused) instead of two SPBs. Subsequently 1NM-PP1 was added to inactivate *mps1-as1*. The *mps1-as1* inactivation did not make the inter-SPB distance larger than that in *MPS1*$^+$ cells (data not shown), probably because sister-kinetochore bi-orientation had been already established prior to this inactivation and was maintained thereafter (see note 4). Our starting cells contained a GFP-marked minichromosome whose sole replication origin was flanked by two recombination sites. Prior to induction of noncleavable Scc1, we removed the replication origin by inducing recombinase from the *MET3* promoter (Figure 4A).

Note 7: Localization of Mps1 Is Not Substantially Altered in an *ipl1* Mutant and vice versa

We studied whether Mps1 and Ipl1 localization is altered in *ipl1* and *mps1* mutants, respectively. First, by using live-cell imaging, we compared localization of GFP-tagged Mps1 in *IPL1*$^+$ and *ipl1-321* cells at 37°C, a restrictive temperature for *ipl1-321* (Figure S7). In the same cells, Mtw1 and Ndc80 were fused with CFP to visualize kinetochores [S16], and Spc42 was fused with RFP to visualize SPBs [S17]. In *IPL1*$^+$ cells with one SPB signal (i.e., cells in G1 or S phase; Figure S7A, top), kinetochore signals overlapped with SPB signals in most cells, and Mps1 signals were found colocalizing with the kinetochore and SPB signals (i.e., with kinetochores at some time points and also with SPBs at the same or other time points; in 76% of cells; 25/33). In *IPL1*$^+$ metaphase cells (Figure S7A, middle and bottom) where SPB signals have separated but not yet segregated to the bud, Mps1 signals colocalized with kinetochore and SPB signals, as previously reported by immunostaining in fixed cells [S18]. The Mps1 localization dynamically changed, and the signals were often found only at kinetochores (Figure S7A, middle) or SPBs (Figure S7A, bottom; Mps1 signals were generally weak and may have not reached the detectable level at both sites). Nonetheless, most (96%; 26/27) of *IPL1*$^+$ metaphase cells showed signals at kinetochores at some time points and also at SPBs at the same or other time points (see Supplemental Experimental Procedures). Thus, Mps1 localized at kinetochores and SPBs, as previously reported [S18]. We found that, in *ipl1-321* cells (Figure S7B), the Mps1 signals still localized at both kinetochores and SPBs (in 79% of cells with one SPB signal, 31/39; in 90% of metaphase cells, 18/20), and the Mps1 signal intensity was not considerably altered, relative to that in *IPL1*$^+$ cells.

We next compared localization of GFP-tagged Ipl1 in *MPS1*$^+$ and *mps1-as1* cells, both treated with 1NM-PP1 following the release from *cdc34-2* arrest (Figure S8). In the same cells, kinetochores (Mtw1, Ctf19, and Ndc80 [S16]) and SPB (Spc42) were visualized with CFP and RFP, respectively. In *MPS1*$^+$ cells with one and two

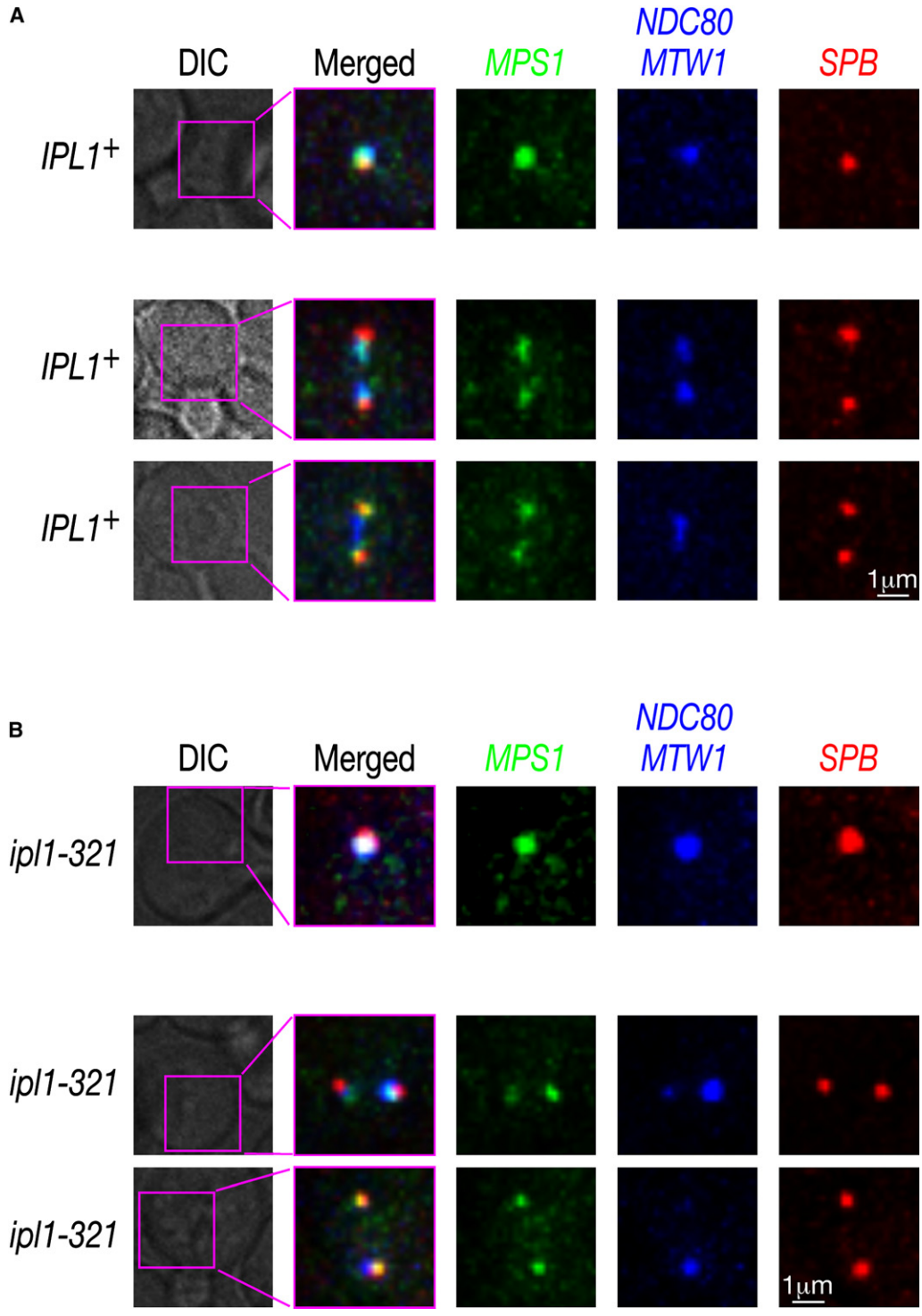

Figure S7. Mps1 Localization Is Not Substantially Altered in *ipl1-321* Mutant Cells

IPL1^{+} (T6108) (A) and *ipl1-321* (T6107) (B) cells with *MPS1-GFP NDC80-3CFP MTW1-3CFP SPC42-RFP* were treated with α factor at 25°C. After 2.5 hr, they were washed and further cultured at 37°C in the absence of α factor. Upon bud emergence and 30 min thereafter, cells were collected to observe Mps1 localization in G1-S phase (top) and in metaphase (middle, bottom), respectively. GFP (green), CFP (blue), and RFP (red) signals were acquired separately every 15 s for 5 min. Representative images are shown.

(but not yet segregated to the bud) SPB signals (Figure S8A), Ipl1 signals colocalized with kinetochore signals (in 96% of cells with one SPB signal, 45/47; in 86% of metaphase cells, 24/28). When SPB signals were separate from kinetochore signals in metaphase cells, Ipl1 colocalized with kinetochores but not with SPBs, which is consistent with the previous reports [S8, S19, S20]. We found that, in *mps1-as1* cells, Ipl1

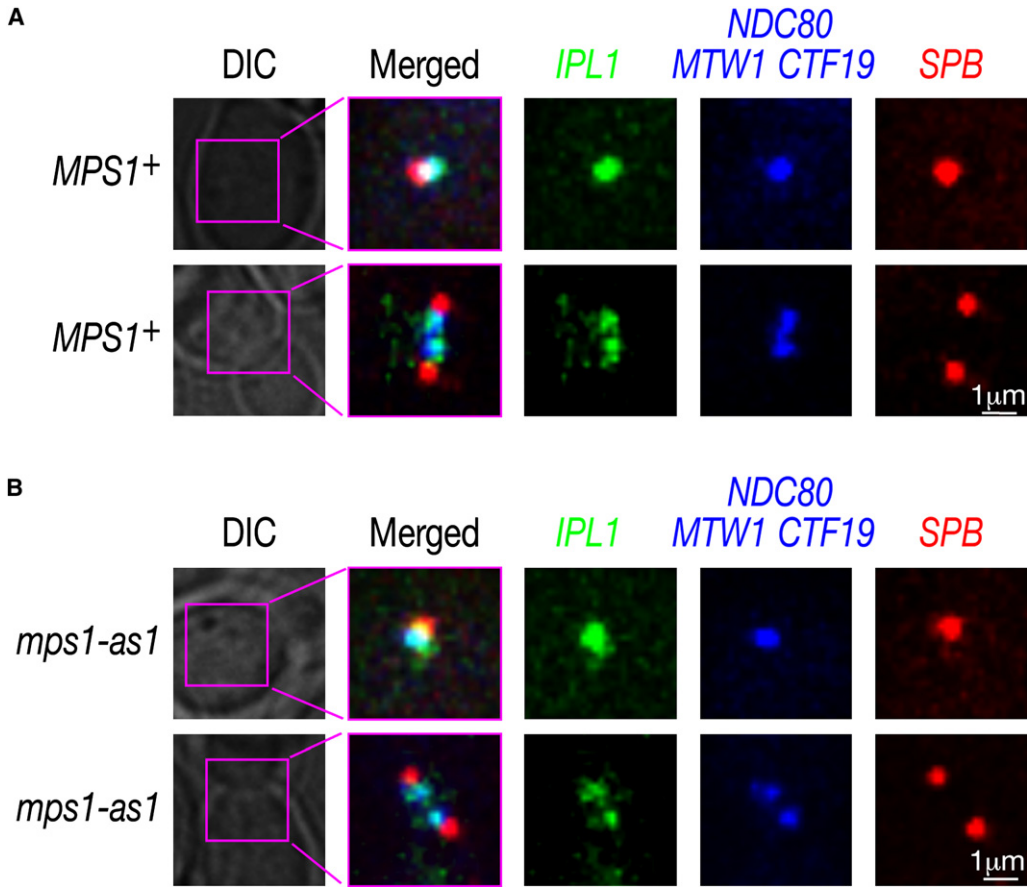

Figure S8. Ipl1 Localization Is Not Substantially Altered in *mps1-as1* Mutant Cells

MPS1^{+} (T5485) (A) and *mps1-as1* (T5481) (B) cells with *cdc34-2 IPL1-GFP NDC80-3CFP MTW1-3CFP CTF19-3CFP SPC42-RFP* were incubated at 37°C for 2.5 hr, leading to arrest because of *cdc34-2*. Subsequently they were incubated at 25°C (to release cells from *cdc34-2* arrest) in the presence of 10 μM 1NM-PP1 (to inactivate *mps1-as1*). After 20 min and 40 min after the washout, cells were collected to observe Mps1 localization in G1-S phase (top) and in metaphase (bottom), respectively. GFP (green), CFP (blue), and RFP (red) signals were acquired separately every 30 s for 10 min. Representative images are shown.

signals still localized at kinetochores (in 94% of cells with one SPB signal, 34/36; in 71% of metaphase cells, 17/24) and Ipl1 signal intensity was not substantially changed (Figure S8B).

Note 8: Mps1 and Ipl1 Kinase Do Not Appear to Regulate Each Other's Kinase Activity

We investigated a possible change in Mps1 and Ipl1 kinase activity in each other's mutant. We immunoprecipitated GFP-tagged Mps1 from *IPL1*$^{+}$ and *ipl1-321* cells at 37°C (*ipl1-321* shows no detectable kinase activity in vitro at this temperature [S21]) and compared the kinase activity in vitro using GST-fused Dam1 as a substrate [S22] (Figure S9A). The *ipl1* mutant did not substantially change the amount of immunoprecipitated Mps1 protein (Figure S9A, bottom) or its kinase activity (Figure S9A, top). Conversely, we immunoprecipitated GFP-tagged Ipl1 from *MPS1*$^{+}$ and *mps1-as1* cells in metaphase, both treated with 1NM-PP1 after the release from *cdc34-2* arrest, and compared the kinase activity in vitro by using GST-fused Dam1 as a substrate [S23] (Figure S9B). The inactivation of Mps1 kinase did not substantially change the amount of immunoprecipitated Ipl1 protein (Figure S9B, bottom) or its kinase activity (Figure S9B, top).

Note 9: The Role of Mps1 in Bi-orientation Is Not Secondary to Its Function in SPB Duplication and Spindle-Assembly Checkpoint

It has been known that Mps1 kinase plays at least two important roles in mitosis [S2]: first, Mps1 is required for the spindle-assembly checkpoint as demonstrated in various organisms including budding yeast [S24, S25]; second, Mps1 is also crucial for duplication of SPBs in budding yeast [S26], although, in humans, there is conflicting evidence regarding Mps1 requirement for centrosome duplication [S27, S28]. How are these two Mps1 functions relevant to its role in sister-kinetochore bi-orientation? Does Mps1 facilitate bi-orientation independently of its function in spindle-assembly checkpoint and SPB duplication? We find that extensive mono-orientation still occurs after Mps1 fulfils its requirement for SPB duplication and is subsequently inactivated. Thus, the role of Mps1 in bi-orientation should be separate from that in SPB duplication. Moreover, the abolishment of the spindle-assembly checkpoint (e.g., by deletion of *MAD2*) does not lead to such extensive mono-orientation in budding yeast [S29]. Indeed, we confirmed that *mad2*-deleted cells do not show a bi-orientation defect on the metaphase spindle (data not shown), after arrest with *cdc34-2* and subsequent

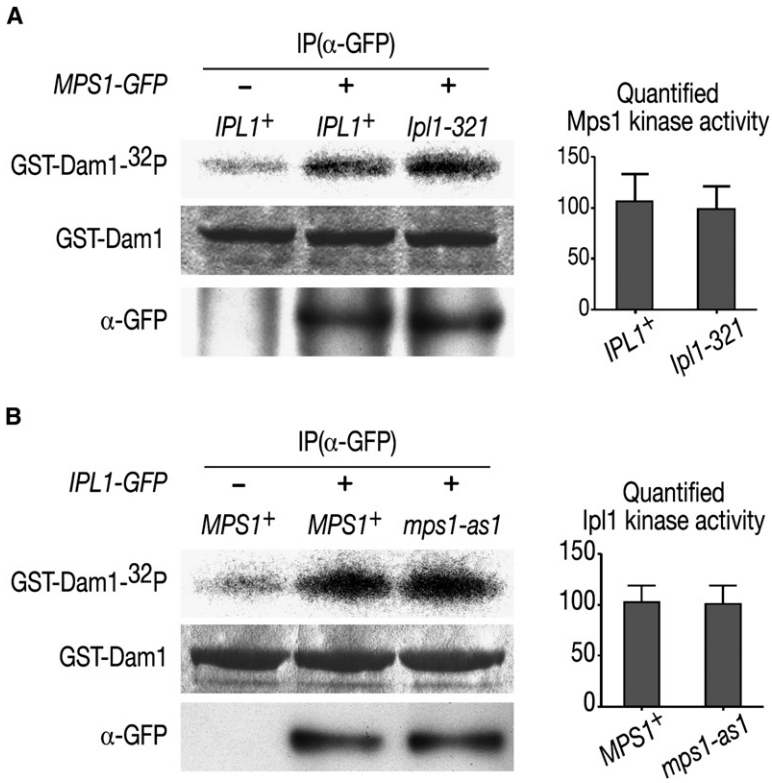

Figure S9. The Kinase Activity of Mps1 Is Not Substantially Altered in *ipl1* Mutant Cells and vice versa

(A) *IPL1*$^+$ cells with *MPS1* (no tag; K699) or *MPS1-GFP* (T5964), and *ipl1-321* cells with *MPS1-GFP* (T5869) were cultured at 37°C for 2 hr and subjected to in vitro kinase assay with GST-Dam1 as a substrate.

(B) *MPS1*$^+$ *IPL1* (no tag; T5901), *MPS1*$^+$ *IPL1-GFP* (T5879), and *mps1-as1 IPL1-GFP* (T5872) cells with *cdc34-2 PMET3-CDC20* were treated as in Figure 2A. 2.5 hr after release from *cdc34-2* arrest, cells were subjected to in vitro kinase assay with GST-Dam1 as a substrate.

In both (A) and (B), ^{32}P-labeled GST-Dam1 (left, top), Coomassie-stained GST-Dam1 (left, middle), and immunoprecipitated GFP fusion proteins (detected by an anti-GFP blot; left, bottom) are shown. Kinase activity was quantified and calibrated (right), as described in Supplemental Experimental Procedures; the graphs show the average and SEM from two (A) and three (B) independent experiments.

release to medium containing 1NM-PP1 (note that *mps1-as1* shows extensive mono-orientation under these conditions). Furthermore, at least one *mps1* mutant allele causes a clear defect in spindle-assembly checkpoint but no growth problem in unperturbed cell culture (therefore no bi-orientation defect) [S18]. Thus, the role of Mps1 in bi-orientation is not secondary to its role in the spindle-assembly checkpoint. On the other hand, given that Mps1 promotes re-orientation of a kinetochore-spindle pole connection (see Figure 4), it may transiently create kinetochores lacking microtubule attachment (as suggested for Ipl1 [S8, S30]), which could then activate the spindle-assembly checkpoint in the absence of tension [S31]. However, the role of Mps1 in the spindle-assembly checkpoint cannot be fully explained by this, because Mps1 is also required to activate the checkpoint when microtubules are depolymerized by nocodazole treatment [S24]. Thus, the role of Mps1 in activating the checkpoint upon loss of microtubule attachment to kinetochores must be independent of its role in bi-orientation.

Note 10: Mps1 Overexpression and Spindle-Assembly Checkpoint Activation

Spindle-assembly checkpoint is activated by cell-cycle perturbation such as spindle disruption or syntelic kinetochore-microtubule attachment where tension is not generated [S15, S32]. Intriguingly, when Mps1 is overexpressed, the spindle-assembly checkpoint is activated without additional cell-cycle perturbation [S33]. Given that Mps1 facilitates detachment of kinetochores from a spindle pole in the absence of tension (see Figure 4), this detachment may happen even for bi-oriented kinetochores when Mps1 is overexpressed, which might lead to spindle-assembly checkpoint activation.

Note 11: Mono-orientation Shows a Bias toward the Bud-Facing SPB when Mps1 Is Inactivated, Similarly to *ipl1* Mutants

Duplication of SPBs takes place in a conservative manner; i.e., the old one, inherited from the previous cell cycle, remains intact while a new one is generated in the present cycle [S34]. In the subsequent anaphase, the old SPB enters the bud while the new one remains in the mother cell body [S35]. We previously found that mono-orientation of sister kinetochores is more frequently formed at the old SPB than at the new SPB, in *ipl1* mutant cells that had undergone DNA replication [S8]. We explained this bias as follows [S8, S36]: centromere DNA replication occurs during early S phase [S37] and might be completed before the new SPB becomes fully functional [S38]. As a result, the majority of nascent kinetochores, assembled on replicated centromeres, might be initially connected to the old SPB even in wild-type cells. When the new SPB becomes functional, re-orientation of kinetochore-spindle pole connections happens between new and old SPBs, facilitated by Ipl1. However, in *ipl1* mutants, the initial connection to the old SPBs would remain. If this explanation were correct, the rate of mono-orientation at the old SPB would decrease in *ipl1* mutants when centromere DNA replication is delayed and more time is given for maturation of the new SPB. We have indeed proven this by comparing the behaviors of early- and late-replicating minichromosomes [S8, S36].

Given that Mps1 facilitates sister-kinetochore bi-orientation with a similar mechanism to Ipl1, one can predict that, when Mps1 is inactivated, mono-orientation of sister kinetochores is also formed more frequently at the old SPB than at the new SPB. However, after Mps1 was inactivated upon release from *cdc34-2* arrest,

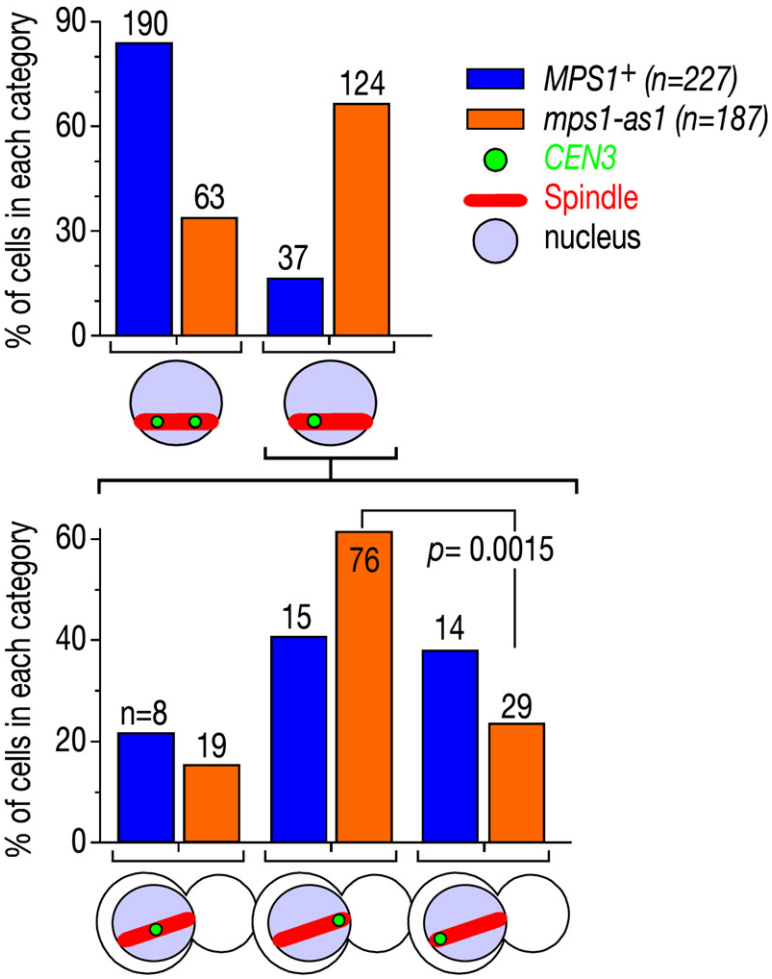

Figure S10. Mono-oriented Centromeres Show a Bias toward the Bud-Facing SPB when Mps1 Was Inactivated after Release from α Factor Arrest

MPS1$^+$ (T3531) and *mps1-as1* (T3869) cells with *PGAL-CEN3-tetOs TetR-GFP YFP-TUB1 PMET3-CDC20* were released from α factor arrest as in Figure S3. At 45 min after this release, 1NM-PP1 was added to inactivate *mps1-as1*. At 180 min after release from α factor arrest, cells were fixed with paraformaldehyde. All media contained glucose, which kept *CEN3* always active during the experiment. Separation and nonseparation of sister *CEN3*s were scored in cells with bipolar spindle (top). In cells with unseparated sister *CEN3*s on bipolar spindle, it was also scored whether *CEN3*s localized in close proximity in either spindle pole or somewhere between the two poles (bottom). n designates the number of samples. p value (0.0015) shown for *mps1-as1* was obtained by comparing 76/29 with 52/52 (i.e., equal distribution of the same number of samples between the two categories) by Fisher's exact test. If we compare the distribution between *MPS1*$^+$ (15/14) and *mps1-as1* (76/29) cells with the same statistic method, p value is 0.044.

mono-orientation was found with similar frequency at the old SPB (the SPB facing the bud during metaphase arrest, assuming that Mps1 inactivation does not change SPB inheritance pattern) and the new SPB (data not shown, Figure 2A), in agreement with a recent report [S3]. We reason that, because *cdc34-2* arrest does not prevent SPB duplication, the new SPB might become functionally mature during this arrest (note that Mps1, required for SPB duplication, is not yet inactivated during the arrest). Thus, after centromere DNA replication after release from *cdc34-2* arrest, kinetochores might be captured with similar frequency by microtubules from the old and new SPBs, leading to mono-orientation equally at the two SPBs.

Such result and consideration prompted us to address possible asymmetry of mono-orientation toward the bud with inactive Mps1, after cells were released from α-factor arrest and rearrested at metaphase by depletion of Cdc20 (Figure S3). When 1NM-PP1 was added 45 min after the release from α-factor arrest, a larger percentage of *mps1-as1* cells showed nonseparated sister *CEN3*s on a bipolar spindle than *MPS1*$^+$ cells, indicative of the defect in bi-orientation (see note 2). In this condition, the new SPB would not become mature before kinetochore capture of microtubules after centromere DNA replication; indeed, *ipl1* mutants showed a bias of mono-orientation toward the old SPB (toward the bud) after release from α-factor arrest [S8]. When Mps1 was inactivated, we indeed found that mono-orientation took place more frequently at a spindle pole facing the bud than at the other pole (Figure S10). We concluded that mono-orientation showed a bias toward the bud when Mps1 was inactive, similarly to *ipl1* mutants.

Note 12: Mps1 Could Promote Re-orientation of Microtubule Kinetochore-Spindle Pole Connections at Kinetochores or at Spindle Poles

Given that bi-orientation is facilitated by re-orientation of kinetochore-spindle pole connections, how does this re-orientation proceed? To complete re-orientation, an old connection must be replaced with a new one. To make a new connection, kinetochores are captured by new microtubules extending from a spindle pole [S39, S40]. How, then, is the old one removed? For this, two different mechanisms are suggested, based on observations in two different types of cells. First, in human HeLa cells, the old connection is abolished at kinetochores, in a step dependent on Aurora B kinase, followed by establishment of the new connection in its place [S41]. Second, in grasshopper spermatocytes, the old connection is released earlier at the spindle pole than at the kinetochore, while a new connection is established at the kinetochore [S42, S43]. Among these steps of re-orientation, which is the one dependent on

the Mps1 kinase? If a new kinetochore-spindle pole connection (replacing an old one) is generated in a similar way to the very initial kinetochore-microtubule interaction, it is unlikely to be dependent on Mps1, which is not required for the very initial interaction (Figure 1B). Instead, Mps1 may be required to remove the old connection. Intriguingly, in contrast to Ipl1 kinase, which localizes at kinetochores but not at SPBs [S19], Mps1 localizes at both kinetochores and spindle poles in budding yeast [S18] (Figure S7); therefore, Mps1 may promote removal of the old connection at either or both of these two sites.

Note 13: Is Dam1 Phosphorylation by either Mps1 or Ipl1 Kinase Important for Bi-orientation?

It has been reported that both Ipl1 and Mps1 phosphorylate Dam1 protein [S22, S23], a key kinetochore component that mediates kinetochore-microtubule interaction in metaphase [S7, S44]. However, the two kinases phosphorylate Dam1 at different sites in the protein [S22, S23]. Are the Dam1 phosphorylations by Ipl1 and Mps1 important for bi-orientation? Dam1 mutants, in which phosphorylation sites by Ipl1 are mutated to mimic constitutive dephosphorylation, are lethal and actually show segregation defects similar to *ipl1* mutants, suggesting that these phosphorylations by Ipl1 are indeed involved in bi-orientation [S23]. On the other hand, Dam1 mutants mimicking constitutive dephosphorylation at Mps1-dependent phosphorylation sites are not lethal and do not show obvious defects in bi-orientation [S22]. Instead, it is suggested that these mutants show defects in coupling kinetochores to microtubule plus ends. Nonetheless, because this coupling could be an important feature of bi-orientation (discussed in [S44]), it is still possible that phosphorylation of Dam1 by Mps1 kinase has an important role in bi-orientation; however, this process might be somehow rescued by Mps1-dependent phosphorylation of other Dam1 complex components or other substrates.

Note 14: How Is the Role of Mps1 in Bi-orientation Evolutionarily Conserved?

Interestingly, the Mps1 ortholog in fission yeast is not an essential gene, and its deletion shows defects in a spindle-assembly checkpoint but not in bi-orientation [S45]. When Mps1 is depleted in human cells, chromosome congression is frequently defective in metaphase, and chromosomes often missegregate in anaphase [S28, S46]. The congression defect might be due to impaired CENP-E loading at kinetochores [S25, S28, S46, S47]; and chromosome missegregation could be due to premature entry into anaphase, caused by an impaired spindle-assembly checkpoint [S2, S25, S48]. However, it is not yet clear whether the bi-orientation defect is also involved in these phenotypes. Comparison of Mps1 function between different organisms will shed more light on the evolution of mechanisms ensuring sister-kinetochore bi-orientation on the mitotic spindle.

Supplemental Experimental Procedures

Yeast Genetics and Molecular Biology

The background of yeast strains (W303), yeast culture media (YP medium, methionine-dropout medium etc.), and methods for α-factor treatment, FACS DNA content analysis, and fixation by paraformaldehyde were as described previously [S44, S49]. The amount of glucose, galactose, and raffinose in culture media was 2%. Constructs of *PGAL-CEN3-tetOs* [S40], *TetR-GFP* [S13], *PMET3-CDC20* [S50], *CEN5-tetO*s (an array of 112 × *tetO*s of 5.6 kb inserted at 1.4 kb left of *CEN5*; [S4]), *TetR-3CFP* [S51], *CEN15-lacO*s (an array of 256 × *lacO*s of 10.1 kb inserted at 1.8 kb left of *CEN15*; [S52]), *GFP-lacI* [S53], *PGAL-SCC1* [S54], *PMET3-R* [S10], and *PGAL-SCC1DD* [S14] were previously described. *SPC42* and *IPL1* were tagged with *RFP* and *GFP*, respectively, at their C termini at their original loci [S8, S55]. *MPS1* was tagged with *GFP* and *NDC80*, *CTF19*, and *MTW1* were tagged with three copies of *CFP* at their C termini at their original loci by a one-step PCR method [S49]. Minichromosomes pT431 and pT323 were constructed as described previously [S8, S10] and introduced to yeast strains by transformation [S49]. Mutant alleles of *mps1-as1* [S3], *cdc34-2* [S56], *ipl1-321* [S57], and *ask1-3* [S58] were previously reported. *YFP-TUB1* plasmid (pDH20, obtained from Yeast Resource Centre, Seattle, WA) were integrated at an auxotroph marker locus. 1NM-PP1 (4-Amino-1-tert-butyl-3-(1′-naphthylmethyl) pyrazolo (3,4-d) pyrimidine) was purchased from Merck Biosciences. Cells were cultured at 25°C in YP medium containing glucose, unless otherwise stated.

Microscopy

The procedures for time-lapse fluorescence microscopy were described previously [S40, S44]. Time-lapse images were collected at 23°C (ambient temperature) unless otherwise stated. For image acquisition, we used a DeltaVision RT microscope (Applied Precision), a UPlanSApo 100 × objective lens (Olympus; NA 1.40), SoftWoRx software (Applied Precision), and either a CoolSnap HQ (Photometrics) or Cascade II 512B (Roper Scientific) CCD camera. We acquired 5–7 (0.7 μm apart) z-sections, which were subsequently deconvoluted, projected to two-dimensional (2D) images, and analyzed with SoftWoRx and Volocity (Improvision) software. GFP and YFP signals were discriminated with the JP3 filter set (Chroma). CFP, YFP, and RFP signals were discriminated with the 89006 filter set (Chroma).

Analyzing Dynamics of Kinetochores and Microtubules

To evaluate the length of microtubules and position of centromeres, we took account of the distance along the z-axis as well as distance on a projected image. In the experiment that studied the behavior of two centromeres (Figure 2A), when both sister centromere signals (separated or nonseparated) were located within 20% of the spindle length from the same SPB (distance was measured between the centers of the two signals), they were scored to be in the vicinity of that SPB as shown by cartoons in the figure. In Figure 2A, a small number of the following cells were categorized in the groups shown in parentheses: cells with both sister *CEN5*s and sister *CEN15*s being located between two SPBs, one or both of them showing nonseparated signals (the left-most category); cells with one pair of sister *CEN*s in the vicinity of an SPB but with the other pair, showing nonseparated signals, between two SPBs (the second category from the left). In the experiment of Scc1 depletion (Figure 2B), when *CEN5* was located within 20% of the spindle length from an SPB, the *CEN5* was scored to be in the vicinity of the SPB. In Figure 2B, the right-most category also included a small number of cells with sister *CEN5* signals nonseparated and being located between two SPBs. The behavior of an unreplicated dicentric minichromosome (mono-oriented or bi-oriented; Figure 3) was scored as follows: when the location of the minichromosome was not more than 20% of the spindle length from an SPB at any consecutive two time points, they were scored as "mono-oriented;" when its location was more than 20% of the spindle length from both SPBs at the majority of time points or it moved vigorously between two SPBs (often with GFP signals stretched), it was scored as "bi-oriented." A small number of cells with the spindle 4 μm or longer were not included in scoring in Figure 3. In the experiment shown in Figure 4, we scored it as re-orientation, when an unreplicated minichromosome moved from the vicinity of one SPB to that of another SPB (here "vicinity of one SPB" meant that the distance from the center of a minichromosome signal to that of a SPB signal was not more than 20% of the distance from the SPB to its closest SPB). In this experiment, the SPB and minichromosome signals overlapped at least partially in the majority

of time points with the signal intensity/contrast used to make the figure. When studying the behavior of an unreplicated minichromosome (Figures 3 and 4), any rare replicated minichromosomes could be distinguished because of the greater intensity of the GFP signal and were not scored. In Figure 4, a small number of cells with five or more SPB signals or with more than one copy of minichromosomes were not included in scoring. In Figures 1B, 3, and 4, *mps1-as1* cells were also treated in the same way but in the absence of 1NM-PP1, as a control; they showed similar phenotypes to *MPS1*$^+$ cells. Appearance of bipolar spindle was scored in Figures S1 and S3, based on the observation of microtubule signals; a monopolar spindle showed a microtubule signal like a comet or a chicken's footprint (where a single or 2–3 microtubules extended from a spindle pole, respectively) whereas a bipolar one showed a microtubule signal like a bipolar rod (or a sausage). In Supplemental Results and Discussion (note 7), colocalization of Mps1-GFP signals with the kinetochore or SPB signals was scored as positive if 80% or more of the GFP-positive area (i.e., above the background level) overlapped with the kinetochore or SPB signals in images projected to 2D at two or more time points out of the initial five time points of time-lapse observation. Colocalization of Ipl1-GFP with the kinetochore signals was also scored in the same way; note that Ipl1-GFP signals, found along microtubules in cells with one SPB signal after release from *cdc34-2* arrest, were not taken into account in scoring colocalization with kinetochores. Statistical analyses in Figures 3C and 4C and Figures S4C, S5B, and S10 were carried out with the Fisher's exact test with the Prism (Graph pad) software. All p values are two-tailed.

In Vitro Kinase Assay

GST-DAM1 was constructed, expressed in *E. coli*, and purified with glutathione sepharose, as described previously [S59]. In vitro kinase assay was carried out as described previously [S20], except that we used an GFP antibody (Roche) to immunoprecipitate GFP-tagged proteins and used GST-Dam1 (5 μg for each condition) as a substrate. 25% and 75% of immunoprecipitated samples were used for kinase assay and a western blot to detect GFP proteins, respectively. Western blots were scanned by a photo-scanner and GFP proteins were quantified with Image J (NIH). ^{32}P-labeled GST-Dam1 was detected and quantified with a phosphorimager (Fuji). The Mps1 kinase activity was quantified and calibrated as follows: the intensity of ^{32}P-labeled GST-Dam1 in cells without GFP tag was subtracted from that in *MPS1-GFP* cells, and the outcome was divided by the intensity of *MPS1-GFP* detected by the GFP antibody; in order to compare results from multiple experiments, this was expressed as the percentage of the averaged value in cells with *IPL1*$^+$ and *ipl1-321*. The Ipl1 kinase activity was also quantified and calibrated in the same way.

Supplemental References

S1. Tanaka, T.U., Stark, M.J., and Tanaka, K. (2005). Kinetochore capture and bi-orientation on the mitotic spindle. Nat. Rev. Mol. Cell Biol. *6*, 929–942.

S2. Winey, M., and Huneycutt, B.J. (2002). Centrosomes and checkpoints: the MPS1 family of kinases. Oncogene *21*, 6161–6169.

S3. Jones, M.H., Huneycutt, B.J., Pearson, C.G., Zhang, C., Morgan, G., Shokat, K., Bloom, K., and Winey, M. (2005). Chemical genetics reveals a role for Mps1 kinase in kinetochore attachment during mitosis. Curr. Biol. *15*, 160–165.

S4. Tanaka, T., Fuchs, J., Loidl, J., and Nasmyth, K. (2000). Cohesin ensures bipolar attachment of microtubules to sister centromeres and resists their precocious separation. Nat. Cell Biol. *2*, 492–499.

S5. Winey, M., Mamay, C.L., O'Toole, E.T., Mastronarde, D.N., Giddings, T.H., Jr., McDonald, K.L., and McIntosh, J.R. (1995). Three-dimensional ultrastructural analysis of the *Saccharomyces cerevisiae* mitotic spindle. J. Cell Biol. *129*, 1601–1615.

S6. Janke, C., Ortiz, J., Lechner, J., Shevchenko, A., Magiera, M.M., Schramm, C., and Schiebel, E. (2001). The budding yeast proteins Spc24p and Spc25p interact with Ndc80p and Nuf2p at the kinetochore and are important for kinetochore clustering and checkpoint control. EMBO J. *20*, 777–791.

S7. Westermann, S., Drubin, D.G., and Barnes, G. (2007). Structures and functions of yeast kinetochore complexes. Annu. Rev. Biochem. *76*, 563–591.

S8. Tanaka, T.U., Rachidi, N., Janke, C., Pereira, G., Galova, M., Schiebel, E., Stark, M.J., and Nasmyth, K. (2002). Evidence that the Ipl1-Sli15 (Aurora kinase-INCENP) complex promotes chromosome bi-orientation by altering kinetochore-spindle pole connections. Cell *108*, 317–329.

S9. Nicklas, R.B., and Koch, C.A. (1969). Chromosome micromanipulation. 3. Spindle fiber tension and the reorientation of mal-oriented chromosomes. J. Cell Biol. *43*, 40–50.

S10. Dewar, H., Tanaka, K., Nasmyth, K., and Tanaka, T.U. (2004). Tension between two kinetochores suffices for their bi-orientation on the mitotic spindle. Nature *428*, 93–97.

S11. Matsuzaki, H., Nakajima, R., Nishiyama, J., Araki, H., and Oshima, Y. (1990). Chromosome engineering in *Saccharomyces cerevisiae* by using a site-specific recombination system of a yeast plasmid. J. Bacteriol. *172*, 610–618.

S12. Hill, A., and Bloom, K. (1987). Genetic manipulation of centromere function. Mol. Cell. Biol. *7*, 2397–2405.

S13. Michaelis, C., Ciosk, R., and Nasmyth, K. (1997). Cohesins: chromosomal proteins that prevent premature separation of sister chromatids. Cell *91*, 35–45.

S14. Uhlmann, F., Lottspeich, F., and Nasmyth, K. (1999). Sister-chromatid separation at anaphase onset is promoted by cleavage of the cohesin subunit Scc1. Nature *400*, 37–42.

S15. Lew, D.J., and Burke, D.J. (2003). The spindle assembly and spindle position checkpoints. Annu. Rev. Genet. *37*, 251–282.

S16. McAinsh, A.D., Tytell, J.D., and Sorger, P.K. (2003). Structure, function, and regulation of budding yeast kinetochores. Annu. Rev. Cell Dev. Biol. *19*, 519–539.

S17. Muller, E.G., Snydsman, B.E., Novik, I., Hailey, D.W., Gestaut, D.R., Niemann, C.A., O'Toole, E.T., Giddings, T.H., Jr., Sundin, B.A., and Davis, T.N. (2005). The organization of the core proteins of the yeast spindle pole body. Mol. Biol. Cell *16*, 3341–3352.

S18. Castillo, A.R., Meehl, J.B., Morgan, G., Schutz-Geschwender, A., and Winey, M. (2002). The yeast protein kinase Mps1p is required for assembly of the integral spindle pole body component Spc42p. J. Cell Biol. *156*, 453–465.

S19. He, X., Rines, D.R., Espelin, C.W., and Sorger, P.K. (2001). Molecular analysis of kinetochore-microtubule attachment in budding yeast. Cell *106*, 195–206.

S20. Buvelot, S., Tatsutani, S.Y., Vermaak, D., and Biggins, S. (2003). The budding yeast Ipl1/Aurora protein kinase regulates mitotic spindle disassembly. J. Cell Biol. *160*, 329–339.

S21. Kotwaliwale, C.V., Frei, S.B., Stern, B.M., and Biggins, S. (2007). A pathway containing the Ipl1/Aurora protein kinase and the spindle midzone protein Ase1 regulates yeast spindle assembly. Dev. Cell *13*, 433–445.

S22. Shimogawa, M.M., Graczyk, B., Gardner, M.K., Francis, S.E., White, E.A., Ess, M., Molk, J.N., Ruse, C., Niessen, S., Yates, J.R., 3rd, et al. (2006). Mps1 phosphorylation of Dam1 couples kinetochores to microtubule plus ends at metaphase. Curr. Biol. *16*, 1489–1501.

S23. Cheeseman, I.M., Anderson, S., Jwa, M., Green, E.M., Kang, J., Yates, J.R., 3rd, Chan, C.S., Drubin, D.G., and Barnes, G. (2002). Phospho-regulation of kinetochore-microtubule attachments by the Aurora kinase Ipl1p. Cell *111*, 163–172.

S24. Weiss, E., and Winey, M. (1996). The *Saccharomyces cerevisiae* spindle pole body duplication gene MPS1 is part of a mitotic checkpoint. J. Cell Biol. *132*, 111–123.

S25. Abrieu, A., Magnaghi-Jaulin, L., Kahana, J.A., Peter, M., Castro, A., Vigneron, S., Lorca, T., Cleveland, D.W., and Labbe, J.C. (2001). Mps1 is a kinetochore-associated kinase essential for the vertebrate mitotic checkpoint. Cell *106*, 83–93.

S26. Winey, M., Goetsch, L., Baum, P., and Byers, B. (1991). MPS1 and MPS2: novel yeast genes defining distinct steps of spindle pole body duplication. J. Cell Biol. *114*, 745–754.

S27. Stucke, V.M., Sillje, H.H., Arnaud, L., and Nigg, E.A. (2002). Human Mps1 kinase is required for the spindle assembly

checkpoint but not for centrosome duplication. EMBO J. *21*, 1723–1732.

S28. Fisk, H.A., Mattison, C.P., and Winey, M. (2003). Human Mps1 protein kinase is required for centrosome duplication and normal mitotic progression. Proc. Natl. Acad. Sci. USA *100*, 14875–14880.

S29. Warren, C.D., Brady, D.M., Johnston, R.C., Hanna, J.S., Hardwick, K.G., and Spencer, F.A. (2002). Distinct chromosome segregation roles for spindle checkpoint proteins. Mol. Biol. Cell *13*, 3029–3041.

S30. Pinsky, B.A., Kung, C., Shokat, K.M., and Biggins, S. (2006). The Ipl1-Aurora protein kinase activates the spindle checkpoint by creating unattached kinetochores. Nat. Cell Biol. *8*, 78–83.

S31. Dorer, R.K., Zhong, S., Tallarico, J.A., Wong, W.H., Mitchison, T.J., and Murray, A.W. (2005). A small-molecule inhibitor of Mps1 blocks the spindle-checkpoint response to a lack of tension on mitotic chromosomes. Curr. Biol. *15*, 1070–1076.

S32. Musacchio, A., and Salmon, E.D. (2007). The spindle-assembly checkpoint in space and time. Nat. Rev. Mol. Cell Biol. *8*, 379–393.

S33. Hardwick, K.G., Weiss, E., Luca, F.C., Winey, M., and Murray, A.W. (1996). Activation of the budding yeast spindle assembly checkpoint without mitotic spindle disruption. Science *273*, 953–956.

S34. Winey, M., and O'Toole, E.T. (2001). The spindle cycle in budding yeast. Nat. Cell Biol. *3*, E23–E27.

S35. Pereira, G., Tanaka, T.U., Nasmyth, K., and Schiebel, E. (2001). Modes of spindle pole body inheritance and segregation of the Bfa1p-Bub2p checkpoint protein complex. EMBO J. *20*, 6359–6370.

S36. Tanaka, T.U. (2005). Chromosome bi-orientation on the mitotic spindle. Philos. Trans. R. Soc. Lond. B Biol. Sci. *360*, 581–589.

S37. McCarroll, R.M., and Fangman, W.L. (1988). Time of replication of yeast centromeres and telomeres. Cell *54*, 505–513.

S38. Lim, H.H., Goh, P.Y., and Surana, U. (1996). Spindle pole body separation in *Saccharomyces cerevisiae* requires dephosphorylation of the tyrosine 19 residue of Cdc28. Mol. Cell. Biol. *16*, 6385–6397.

S39. Rieder, C.L., and Alexander, S.P. (1990). Kinetochores are transported poleward along a single astral microtubule during chromosome attachment to the spindle in newt lung cells. J. Cell Biol. *110*, 81–95.

S40. Tanaka, K., Mukae, N., Dewar, H., van Breugel, M., James, E.K., Prescott, A.R., Antony, C., and Tanaka, T.U. (2005). Molecular mechanisms of kinetochore capture by spindle microtubules. Nature *434*, 987–994.

S41. Hauf, S., Cole, R.W., LaTerra, S., Zimmer, C., Schnapp, G., Walter, R., Heckel, A., Van Meel, J., Rieder, C.L., and Peters, J.M. (2003). The small molecule Hesperadin reveals a role for Aurora B in correcting kinetochore-microtubule attachment and in maintaining the spindle assembly checkpoint. J. Cell Biol. *161*, 281–294.

S42. Nicklas, R.B., and Kubai, D.F. (1985). Microtubules, chromosome movement, and reorientation after chromosomes are detached from the spindle by micromanipulation. Chromosoma *92*, 313–324.

S43. Ault, J.G., and Nicklas, R.B. (1989). Tension, microtubule rearrangements, and the proper distribution of chromosomes in mitosis. Chromosoma *98*, 33–39.

S44. Tanaka, K., Kitamura, E., Kitamura, Y., and Tanaka, T.U. (2007). Molecular mechanisms of microtubule-dependent kinetochore transport toward spindle poles. J. Cell Biol. *178*, 269–281.

S45. He, X., Jones, M.H., Winey, M., and Sazer, S. (1998). Mph1, a member of the Mps1-like family of dual specificity protein kinases, is required for the spindle checkpoint in *S. pombe*. J. Cell Sci. *111*, 1635–1647.

S46. Liu, S.T., Chan, G.K., Hittle, J.C., Fujii, G., Lees, E., and Yen, T.J. (2003). Human MPS1 kinase is required for mitotic arrest induced by the loss of CENP-E from kinetochores. Mol. Biol. Cell *14*, 1638–1651.

S47. Kapoor, T.M., Lampson, M.A., Hergert, P., Cameron, L., Cimini, D., Salmon, E.D., McEwen, B.F., and Khodjakov, A. (2006). Chromosomes can congress to the metaphase plate before biorientation. Science *311*, 388–391.

S48. Meraldi, P., Draviam, V.M., and Sorger, P.K. (2004). Timing and checkpoints in the regulation of mitotic progression. Dev. Cell *7*, 45–60.

S49. Amberg, D.C., Burke, D.J., and Strathern, J.N. (2005). Methods in Yeast Genetics (Cold Spring Harbor, NY: Cold Spring Harbor Laboratory Press).

S50. Uhlmann, F., Wernic, D., Poupart, M.A., Koonin, E.V., and Nasmyth, K. (2000). Cleavage of cohesin by the CD clan protease separin triggers anaphase in yeast. Cell *103*, 375–386.

S51. Bressan, D.A., Vazquez, J., and Haber, J.E. (2004). Mating type-dependent constraints on the mobility of the left arm of yeast chromosome III. J. Cell Biol. *164*, 361–371.

S52. Goshima, G., and Yanagida, M. (2000). Establishing biorientation occurs with precocious separation of the sister kinetochores, but not the arms, in the early spindle of budding yeast. Cell *100*, 619–633.

S53. Straight, A.F., Belmont, A.S., Robinett, C.C., and Murray, A.W. (1996). GFP tagging of budding yeast chromosomes reveals that protein-protein interactions can mediate sister chromatid cohesion. Curr. Biol. *6*, 1599–1608.

S54. Uhlmann, F., and Nasmyth, K. (1998). Cohesion between sister chromatids must be established during DNA replication. Curr. Biol. *8*, 1095–1101.

S55. Maekawa, H., Usui, T., Knop, M., and Schiebel, E. (2003). Yeast Cdk1 translocates to the plus end of cytoplasmic microtubules to regulate bud cortex interactions. EMBO J. *22*, 438–449.

S56. Schwob, E., Bohm, T., Mendenhall, M.D., and Nasmyth, K. (1994). The B-type cyclin kinase inhibitor p40SIC1 controls the G1 to S transition in *S. cerevisiae*. Cell *79*, 233–244.

S57. Biggins, S., Severin, F.F., Bhalla, N., Sassoon, I., Hyman, A.A., and Murray, A.W. (1999). The conserved protein kinase Ipl1 regulates microtubule binding to kinetochores in budding yeast. Genes Dev. *13*, 532–544.

S58. Li, Y., and Elledge, S.J. (2003). The DASH complex component Ask1 is a cell cycle-regulated Cdk substrate in *Saccharomyces cerevisiae*. Cell Cycle *2*, 143–148.

S59. Pinsky, B.A., Kotwaliwale, C.V., Tatsutani, S.Y., Breed, C.A., and Biggins, S. (2006). Glc7/protein phosphatase 1 regulatory subunits can oppose the Ipl1/aurora protein kinase by redistributing Glc7. Mol. Cell. Biol. *26*, 2648–2660.